ACS BIO & MED CHEM Au
AN OPEN ACCESS JOURNAL OF THE AMERICAN CHEMICAL SOCIETY

pubs.acs.org/biomedchemau

Article

Template-Based Porous Hydrogel Microparticles as Carriers for Therapeutic Proteins

Philippe Delbreil, Xavier Banquy, and Davide Brambilla*

Cite This: *ACS Bio Med Chem Au* 2023, 3, 252−260

Read Online

ACCESS | Metrics & More | Article Recommendations | Supporting Information

ABSTRACT: Hydrogels have been extensively researched for over 60 years for their limitless applications in biomedical research. In this study, porous hydrogel microparticles (PHMPs) made of poly(ethylene glycol) diacrylamide were investigated for their potential as a delivery platform for therapeutic proteins. These particles are made using hard calcium carbonate ($CaCO_3$) templates, which can easily be dissolved under acidic conditions. After optimization of the synthesis processes, both $CaCO_3$ templates and PHMPs were characterized using a wide range of techniques. Then, using an array of proteins with different physicochemical properties, the encapsulation efficiency of proteins in PHMPs was evaluated under different conditions. Strategies to enhance protein encapsulation via modulation of particle surface charge to increase electrostatic interactions and conjugation using EDC/NHS chemistry were also investigated. Conjugation of bovine serum albumin to PHMPs showed increased encapsulation and diminished release over time, highlighting the potential of PHMPs as a versatile delivery platform for therapeutic proteins such as enzymes or antibodies.

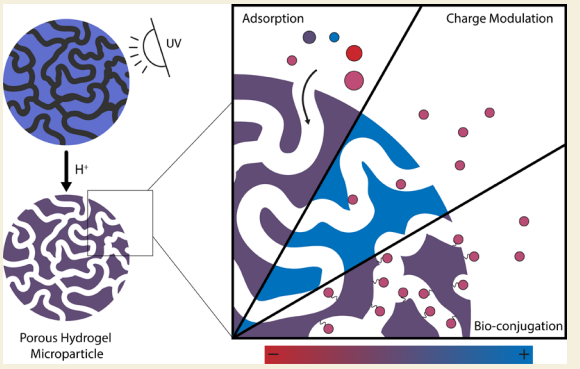

KEYWORDS: *hydrogel, template, porous, microparticles, protein delivery, bioconjugation*

INTRODUCTION

Since the first report in 1960 by Wichterle and Lím, which led to the ground-breaking introduction of soft contact lenses in 1971, hydrogels have been extensively researched in a wide variety of fields including drug delivery, tissue repair, diagnostics, cosmetics, and even agriculture.[1−4] These water-swollen networks obtain their structure from chemical or physical cross-linking of hydrophilic polymers from natural or synthetic sources. By tuning properties such as polymer composition or cross-link density, hydrogels can be engineered to obtain ideal mechanical and chemical properties for a wide range of applications. Their size and shape can also be adapted to the delivery route, such as macroscopic gels for subdermal implantation,[5] microgels for oral delivery,[6] or nanogels for systemic administration.[7] Furthermore, their high water content (up to 99%) grants them structural similarity with most biological tissues and can enhance their biocompatibility and drug loading potential.[8] In this regard, poly(ethylene glycol) (PEG) hydrogels have seen a lot of interest due to their versatility and high biocompatibility.[9] PEG is a hydrophilic, nonionic polymer, which can easily be coupled to other molecules or proteins for therapeutic use. As drug delivery platforms, PEG hydrogels can be engineered to release a therapeutic agent in a controlled or stimuli-responsive manner and protect it from degradation.[10]

To further enhance drug loading potential, hydrogels can be made porous using a wide variety of methods such as the commonly used cryogelation,[11] gas foaming,[12] or micro-emulsion templating.[13,14] In fact, porous hydrogels present many advantages for drug delivery, such as modifying the mechanical properties,[8,11] accommodating large payloads (e.g., cells or large proteins),[3,15] and allowing for a high encapsulation potential of therapeutic agents due to their increased specific surface area.[16]

In this study, we investigated the potential of porous hydrogel microparticles (PHMPs) to act as carriers for proteins. Based on previous work,[17] we used hard templating to create an interconnected network of pores within a poly(ethylene glycol) diacrylamide (PEG-dAAm) hydrogel network. The templates are made from precipitation of calcium carbonate ($CaCO_3$) into vaterite microspheres, which can then easily be dissolved under acidic conditions. Their synthesis was optimized to obtain ideal sample morphology and maximize porosity for further PHMP fabrication. The PHMPs were also

Received: January 11, 2023
Revised: February 24, 2023
Accepted: February 27, 2023
Published: March 10, 2023

https://doi.org/10.1021/acsbiomedchemau.3c00001
ACS Bio Med Chem Au 2023, 3, 252−260

optimized by evaluating the influence of polymer molecular weight on particle morphology and yield. We then used an array of techniques to characterize both the templates and the PHMPs and used proteins of different sizes and isoelectric points to evaluate encapsulation efficiency (EE) into the PHMPs. Finally, we investigated potential strategies to optimize protein encapsulation and release through modulation of PHMP charge or protein conjugation. Our findings may help provide a better understanding of protein−hydrogel interactions and lead to an interesting delivery platform for enzymes, antibodies, and other therapeutic proteins for diverse biomedical applications.

MATERIALS AND METHODS

Materials

PEG-dAAm 3.7 kDa, 1-ethyl-3-(3-dimethyl-aminopropyl) carbodiimide hydrochloride (EDC), 2-mercaptoethanol, 2-(*N*-morpholino)-ethanesulfonic acid (MES), phenylalanine ammonia lyase (PAL), glucose oxidase (GOx), avidin-FITC, IgG-FITC, and bovine serum albumin (BSA)-FITC were purchased from Sigma-Aldrich. Sodium carbonate ($NaCO_3$), calcium chloride ($CaCl_2$), *N*-hydroxysuccinimide (NHS), sodium bicarbonate ($NaHCO_3$), and hydrochloric acid (HCl) were purchased from Fisher Scientific. Irgacure 2959 was purchased from BASF. Acrylate-PEG-NH-Boc MW 2 kDa and PEG-dAAm (0.6, 2, 10, and 20 kDa) were purchased from Creative PEGWorks. Cy5-NHS was synthesized as previously reported.[18]

$CaCO_3$ Template Synthesis

Template microparticles of calcium carbonate were synthesized by mixing solutions of sodium carbonate ($NaCO_3$) and calcium chloride ($CaCl_2$) at concentrations ranging from 0.1 to 0.8 M and temperatures ranging from 5 to 40 °C. The solutions were mixed by adding 400 mL of $NaCO_3$ to 400 mL of $CaCl_2$ in a glass beaker and stirring at 650 rpm for 30 s. After agitation, the mixture was filtered over a Whatman paper filter (grade 42) and rinsed with water. Finally, the resulting white paste was moved to a watch glass and left to air dry for at least 4 h.

$CaCO_3$ Template Characterization

$CaCO_3$ template size and morphology were evaluated by optical microscopy using a Zeiss Axio Zoom V16 microscope and Zeiss ZEN Blue software. Porosity was evaluated by measuring the density of the dry powder with an Ultrapycnometer 1000 (Quantachrome Instruments, Boynton Beach, Florida) and comparing it to the density of the bulk material.

PEG-dAAm Synthesis

PEG-dAAm PHMPs were synthesized by adapting a protocol previously reported by Behra et al.[17] Thirty milligrams of PEG-dAAm and 150 mg of $CaCO_3$ templates were mixed with 375 μL of a 4 mg/mL Irgacure 2959 solution (photoinitiator) in a 1.5 mL Eppendorf tube. The mixture was gently mixed for 30 min in the dark before being transferred to a 10 mL round-bottom flask. The flask was placed on a rotary evaporator and water was removed by setting the temperature and pressure at 80 °C and 90 mbar, respectively, for 90 min. The flask was then left open at 70 °C to remove any remaining moisture, cooled to room temperature, and 12−15 mL of diethyl ether was added, as well as a small magnetic bar for stirring. Under the effect of stirring, while also gently scraping the walls of the flask using a spatula, the PEG-dAAm and photoinitiator-loaded $CaCO_3$ templates were resuspended in diethyl ether. When a homogenous suspension was formed, the flask (closed) was put under UV light for 90 s twice with a 60 s break in between. The suspension was then stirred for an additional 5 min to ensure no aggregation.

The solvent was removed by centrifugation for 5 min at 400 *g*, and the remaining pellet was left to dry under a fume hood for a few minutes. The particles were washed with water by centrifugation using the same settings. Then, the templates were removed by addition of 3 mL of 1 N HCl. The PHMPs were then washed with water at least two times and once with the desired resuspension buffer (phosphate buffered saline (PBS), phosphate buffer (PB), and citrate) by centrifugation at 500 *g* for 20 min. Finally, particles were resuspended in the desired amount of buffer and stored at 4 °C.

Protein Labeling

Among the proteins investigated, avidin, BSA, and IgG were purchased already labeled with a fluorescent dye. PAL and GOx were labeled with cy5 using the following protocol: 150 μL of PAL stock solution (7.1 mg/mL) was dialyzed overnight at 4 °C in 0.1 M sodium bicarbonate (pH 8.5) using a Thermo Scientific Slide-A-Lyzer dialysis cassette (0.5 mL, 10,000 MWCO) to remove glycerol and Tris buffer. The protein was recovered and 3 μL of Cy5-NHS (3 mg/mL in DMSO) was added and incubated overnight at 4 °C. The labeled protein was purified using a column with Sephadex G-15 (Cytiva). The absence of free dye was confirmed using thin layer chromatography with a water/methanol 1:9 mixture as the mobile phase.

The same protocol was used for GOx, without initial dialysis, as it is provided as a lyophilized powder.

The concentration of labeled proteins was assessed by measuring the absorbance at 280 nm and 646 nm (λ_{max} of cy5) in a quartz 96-well plate (volume 350 μL for a 1 cm light path). The following formula was then used to calculate labeled protein concentration:

$$\text{Protein concentration } (M) = \frac{A_{280\text{ nm}} - (A_{646\text{ nm}} \times \text{CF})}{\varepsilon} \times \text{dilution factor}$$

where ε is the protein molar extinction coefficient and CF is the correction factor for the dye.

Protein Loading

For quantification of protein EE, particles were counted using a hematocytometer. The appropriate volume to obtain three million (*M*) particles was mixed with 50 μL of a 320 μg/mL solution of the desired fluorescently labeled protein and buffer of interest to a final volume of 400 μL for a final protein concentration of 40 μg/mL. Controls were prepared the same way without addition of MPs (final volume 400 μL and 40 μg/mL protein). Then, the samples were gently mixed for 45 min. The tubes were then centrifuged at 2500 *g* for 20 min, and the supernatant was collected and diluted 4× and quantified by measuring the fluorescence in a 384-well plate using a TECAN Spark multimode microplate reader.

Particle Charge Modulation

The surface charge of PHMPs was modified by addition of 2-(methacryloyloxy)ethyl-trimethylammonium chloride (MAETAC) at concentrations of 200 and 300 mM at the start of PHMP synthesis. For the second strategy, 2-(dimethylamino)ethyl methacrylate (DMAEMA) was added at a concentration of 200 mM at the start of the synthesis. After the synthesis, PHMPs were resuspended in acetone with ethyl bromide (0.5 M) and left to react for 24 h. The PHMPs were then washed several times to exchange acetone for PBS. For inclusion of an amine, PHMPs were synthesized as described above and adding 2.5% or 5 mol % of acrylate-PEG-NH-Boc. At the end of the synthesis, the amine groups were deprotected by resuspending the PHMPs in 4 M HCl for at least 2 h and washing three times by centrifugation in a large volume (12 mL).

Zeta potential was measured in PBS by phase analysis light scattering (PALS) using a Brookhaven Instruments NanoBrook zeta potential analyzer.

Protein Conjugation

Two methods of functionalization were tested. Method one consisted in grafting a carboxyl group to the PEG backbone on the PHMPs by adapting a procedure previously reported.[19,20] To do this, the water of the PHMP suspension was exchanged for ethanol through two centrifugation cycles. Then, benzophenone and crotonic acid were added to concentrations of 25 and 150 mg/mL (for a final volume of 2 mL of ethanol), respectively. The suspension was flushed with

https://doi.org/10.1021/acsbiomedchemau.3c00001
ACS Bio Med Chem Au 2023, 3, 252−260

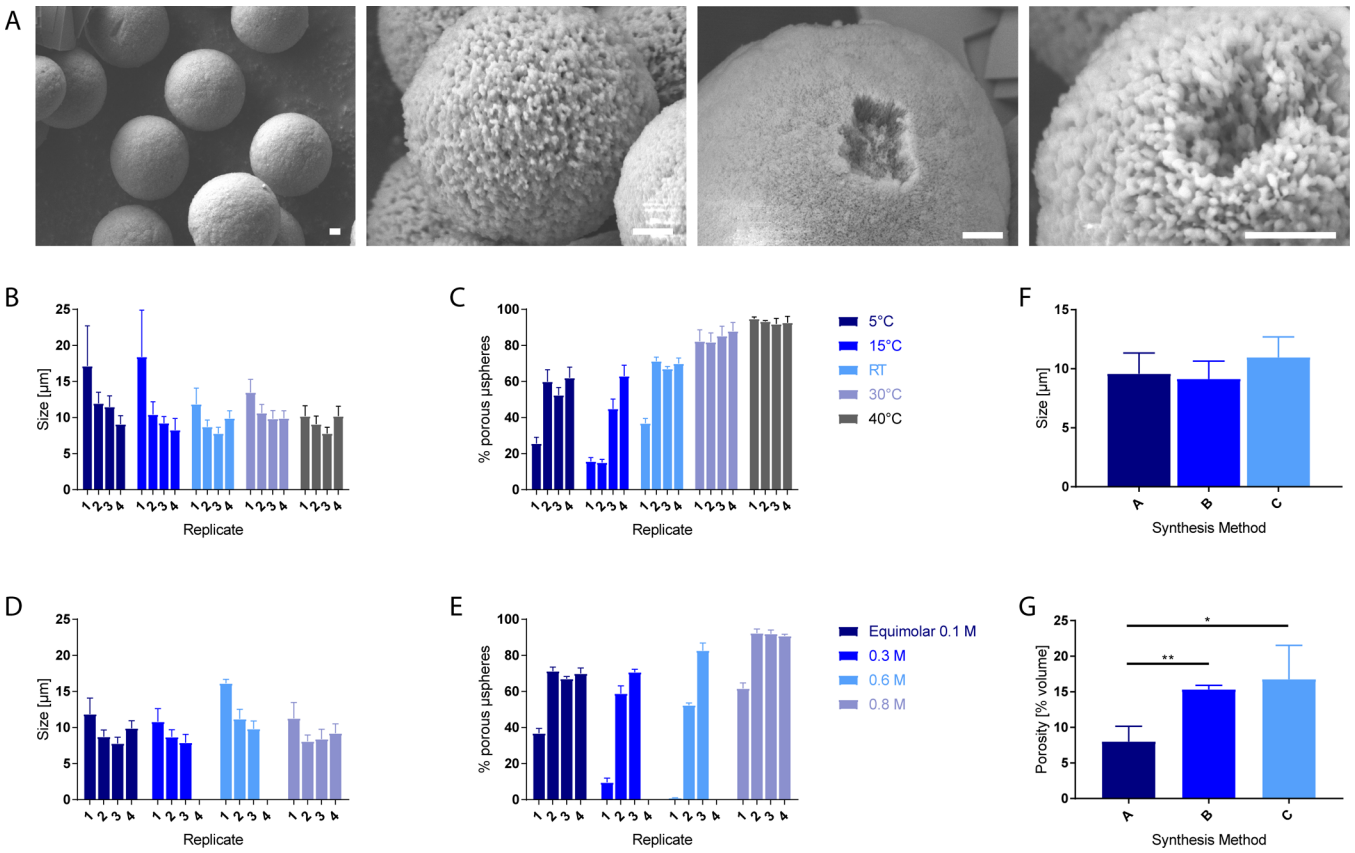

Figure 1. Optimization of $CaCO_3$ templates. (A) SEM images of spherical templates with visible inner porosity (from synthesis method C). (B, C) Effect of temperature on size and morphology of templates in consecutive syntheses. (D, E) Effect of $NaCO_3$ concentration on size and morphology of templates in consecutive syntheses. (F, G) Size of templates from three different synthesis parameters and corresponding porosity. A: RT, equimolar concentrations, B: 30 °C, equimolar concentrations, and C: RT, 0.3 M $NaCO_3$, 0.1 M $CaCl_2$. Data presented as mean ± SD ($n \geq 3$). Scale bars represent 1 μm.

nitrogen for 30 s and irradiated with UV light for 15 min. The PHMPs were then washed twice with 15 mL of ethanol, and the medium was exchanged for 0.1 M MES buffer (pH 5.5) through two additional centrifugation steps. A weight of 0.4 mg of EDC and 0.6 mg of NHS were added per 1 mL of suspension, which was left at room temperature for 15 min to react. The PHMPs were washed once with water and resuspended in a 0.5 mg/mL protein solution in 0.1 M sodium bicarbonate. The modified PHMPs and protein were left to react for 2 h at room temperature.

For method two, a primary amine was introduced in the PHMP structure and coupled to the carboxyl group on the protein. First, the PHMPs were synthesized using the above-described protocol and adding 5 mol % of acrylate-PEG-NH-Boc. The amine groups were then deprotected by resuspending the PHMPs in 4 M HCl for 2 h and washing three times with water by centrifugation (400 *g*, 20 min). For the final centrifugation, the PHMPs were resuspended in PBS pH 7.4.

In parallel, 0.4 mg of EDC and 0.6 mg of NHS were added to 1 mL of a 5 mg/mL protein solution in ultrapure water and left to react at room temperature for 15 min. Then, 1.4 μL of 2-mercaptoethanol was added to neutralize unreacted EDC, followed by an appropriate amount of concentrated PBS (10×) to reach pH 7.4. The modified PHMPs and the activated protein were then mixed, at a protein concentration of 100 μg/mL, and allowed to react overnight at RT.

Quantification of Conjugated Protein Encapsulation and Release

After the conjugation, the PHMPs (in a 1.5 mL tube) were centrifuged at 2500 *g* for 20 min. The supernatant was collected and diluted 10× and quantified by measuring the fluorescence in a 384-well plate.

For quantification of protein release, the samples were resuspended in 1 mL of PBS after removal of the supernatant for quantification of protein encapsulation. Then, at every time point, samples were centrifuged and 100 μL was removed for quantification and replaced by PBS.

Statistical Analysis

All data in this study are presented as mean ± standard deviation (SD). For comparison of two data sets, significance of the presented results was determined by using a Mann−Whitney nonparametric *t* test or a parametric Student's *t* test with Welch's correction and a *p* value <0.05. Significance of results is indicated by (*) $p \leq 0.05$; (**) $p \leq 0.01$; (***) $p \leq 0.001$; and (****) $p < 0.0001$. Statistical analysis and graph plotting were done using GraphPad Prism 7 software.

RESULTS AND DISCUSSION

Optimization of $CaCO_3$ Templates

While many methods have been reported for accurate control of $CaCO_3$ precipitation, such as the most common industrial method of CO_2 bubbling in a calcium solution, these methods often require extreme conditions or specialized equipment.[21] In this study, $CaCO_3$ templates used for the synthesis of PHMPs were made by mixing two salt solutions ($CaCl_2$ and $NaCO_3$), which led to spherical microparticles with interconnected pores, as observed by scanning electron microscopy (SEM) (Figure 1A). However, this procedure has shown to yield highly variable results and poor reproducibility without precise control of synthesis parameters.

https://doi.org/10.1021/acsbiomedchemau.3c00001
ACS Bio Med Chem Au 2023, 3, 252−260

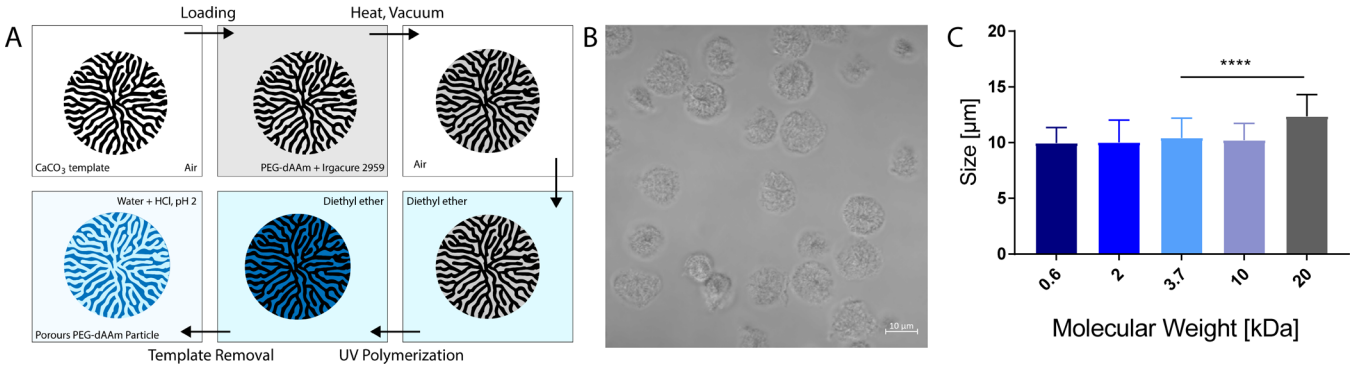

Figure 2. Synthesis of PEG-dAAm porous microspheres. (A) Schematic representation of the synthetic procedure of PHMPs via hard templating (adapted with permission from Behra et al.,[17] "Synthesis of Porous PEG Microgels Using $CaCO_3$ Microspheres as Hard Templates", 2012, *Macromol. Rapid Commun.*, Copyright 2012 WILEY-VCH Verlag GmbH & Co. KGaA, Weinheim). (B) DIC microscopy images of PHMPs (3.7 kDa). (C) Influence of polymer molecular weight on the diameter of PHMPs. Data presented as mean ± SD ($n \geq 3$).

The two main outcome criteria taken into consideration for the optimization of these templates were the size of the particles and the percentage of porous microspheres. For optimal results in the synthesis of PHMPs, template samples should have a mean diameter in the range of 5 to 15 μm and no less than 70% of porous microspheres. The latter parameter refers to the different $CaCO_3$ morphologies that can be obtained, which include vaterite, calcite, and aragonite.[22] In our experiments, we only observed the formation of vaterite and calcite (nonporous rhomboids, Figure S1A). While previous works focused on the optimization of template fabrication and identified different factors influencing the size of vaterite microspheres such as stirring speed and time as well as salt concentration,[23,24] we also observed that some samples contained almost exclusively rhombohedral, nonporous calcite, which needed to be addressed during optimization. While the process of PHMP synthesis is not affected by the presence of calcite, its presence does decrease the yield of the procedure and should ideally be kept to a minimum (<30%). Therefore, the influence of temperature and $NaCO_3$ concentration (an excess of which has been reported to favor vaterite formation[25]) while maintaining identical agitation speed and time (650 rpm for 30 s) was investigated. As every parameter was evaluated at least in triplicates, it was revealed that both size and morphology of templates varied between replicates (Figure 1B–E). In fact, consecutive syntheses in the same glassware, rinsed with ultrapure water between replicates, seemed to generally decrease particle size and increase the percentage of porous microspheres. This phenomenon could be explained by the residual $CaCO_3$ deposits on glassware (Figure S1B), which could favor vaterite formation by acting as seeds controlling the nucleation reaction. In fact, previous works using such seeds have reported higher rates of vaterite formation over other forms of $CaCO_3$.[26−28] These deposits build up on glass through interfacial interactions[29] after each synthesis and can only be cleaned off the glass surface with the use of an acidic solution, which reacts with $CaCO_3$ to create carbon dioxide (CO_2) and water-soluble calcium chloride ($CaCl_2$).[30]

From these data, the porosity of samples from three synthesis methods yielding optimal templates (A: RT, equimolar concentrations, B: 30 °C, equimolar concentrations, and C: RT, 0.3 M $NaCO_3$, 0.1 M $CaCl_2$) was evaluated by comparing the density of synthesized template samples to the density of the bulk material (2.71 g/cm^3). Both methods B and C yielded a significantly higher degree of porosity than method A (Figure 1F,G), and method C was chosen as the standard method for further experiments as it also had the highest proportion of porous microspheres (83 vs 71% for method B). Overall, the synthesis of $CaCO_3$ templates was optimized to obtain a reproducible size and morphology, which could be used for further synthesis of PHMPs.

Porous Hydrogel Microparticle Synthesis

Using the $CaCO_3$ microparticles as templates, PHMPs were synthesized following an adaptation of the protocol previously described by Behra et al.[17] (Figure 2A). These particles are made of PEG-dAAm, which undergoes free-radical polymerization upon exposure to UV light. Due to their transparency in aqueous suspensions, differential interference contrast (DIC) microscopy is favored over optical microscopy for their observation (Figure 2B). As polymer molecular weight can affect the structural properties of hydrogels such as the swelling degree,[31,32] we investigated a wide range of molecular weights to evaluate their influence on particle morphology. A molecular weight of 3.7 kDa showed the highest yield and best overall morphology (few aggregates and uniform sample of spherical particles) of all molecular weights. Furthermore, particle size was not affected by the molecular weight, with the exception of 20 kDa, which displayed a higher particle diameter than 3.7 kDA (Figure 2C). However, high degrees of aggregation and loss of spherical morphology were also observed at higher molecular weights (Figure S2), which could lead to increased particle sizes. It could be hypothesized that the higher viscosity of high molecular weight polymer solutions[33] impedes the proper diffusion of the polymer within the pores of the templates, leading to particles of lesser quality. These data suggest that $CaCO_3$ template size rather than the molecular weight of polymers governs PHMP size and that a molecular weight of 3.7 kDa yields optimal results.

Additionally, standard and low vacuum SEM was attempted to observe the porous surface of these PHMPs. The results showed a loss of structural integrity following freezing or drying, as well as damage to the particles from the electron beam (Figure S3). Finally, to evaluate any potential electrostatic interactions with proteins in further experiments, the zeta potential of PHMPs was measured at −2.2 mV, displaying a slightly negative, near-neutral surface charge.

https://doi.org/10.1021/acsbiomedchemau.3c00001
ACS Bio Med Chem Au 2023, 3, 252−260

Protein Encapsulation

The encapsulation of proteins with different properties (Table 1) was evaluated to assess PHMP potential for delivery of biologics such as enzymes or antibodies. Using confocal microscopy, multiple fluorescence images were captured at different points on the Z-axis (Z-stack) and used to create a three-dimensional reconstruction to visualize protein adsorption in the PHMPs (Figure 3A). From these images, it can be observed that all proteins investigated with the exception of GOx were adsorbed throughout the whole particle, also confirming the porous nature of the PHMPs.

Table 1. Molecular Weights and Isoelectric Points of Proteins Evaluated for Encapsulation

Protein	Size (kDA)	pI
BSA[34,35]	66	4.7
avidin[36]	67	10.5
IgG[37]	150	6.5−9.5
GOx[38]	160	4.2
PAL[39]	330	5.4

Quantification of protein adsorption was done by measuring the EE of PHMPs in a 40 μg/mL protein solution in ultrapure water (pH 6.9) and three different buffers. Among these buffers were PBS and PB, two buffers at physiological pH (7.4) with one of the two being saline, as the presence of salts in buffer has been shown to interfere with noncovalent interactions between proteins and hydrogels as well as the hydrogel structure itself.[40−42] We also chose citrate buffer (pH 5.4) to evaluate if a change in overall protein charge would affect EE. As some proteins have an isoelectric point (pI) above or equal to 5.4 (Table 1), and PHMPs have a near-neutral, slightly negative zeta potential (−2.2 mV), this could favor electrostatic interactions between the two.

Overall, EE is highest in water for all proteins, which can be expected, as greater ionic strength, among other factors, has been reported to reduce protein adsorption to PEGylated surfaces[40] (Figure 3B). PAL showed the highest EE at nearly 75% for the conditions tested, followed by IgG (43%), avidin (28%), BSA (23%), and GOx (6.5%). At physiological pH, EE did not differ significantly between saline and nonsaline buffers for all proteins evaluated with the exception of PAL. Indeed, PAL EE was 38% in PB and 16% in PBS, suggesting that the presence of salts impeded PAL adsorption in the PHMPs. For all other proteins, EE at physiological pH was generally low (≤10%) and showed no significant difference between PB and PBS. At pH 5.4, EE was significantly improved for PAL compared to pH 7.4, but this was not the case for other proteins. As the pI of PAL is 5.4 (Table 1), its overall neutral charge at this pH could increase nonspecific interactions with the PHMPs. Avidin and GOx, with lower pIs of 4.7 and 4.2, respectively, would still have an overall negative charge at pH 5.4 and would therefore not show an increase in EE. As observed through confocal microscopy, GOx presented drastically different EE results, as no protein encapsulation was measurable for all three buffers evaluated, and only 6.5% EE was obtained in water, which is significantly lower than all other proteins investigated.

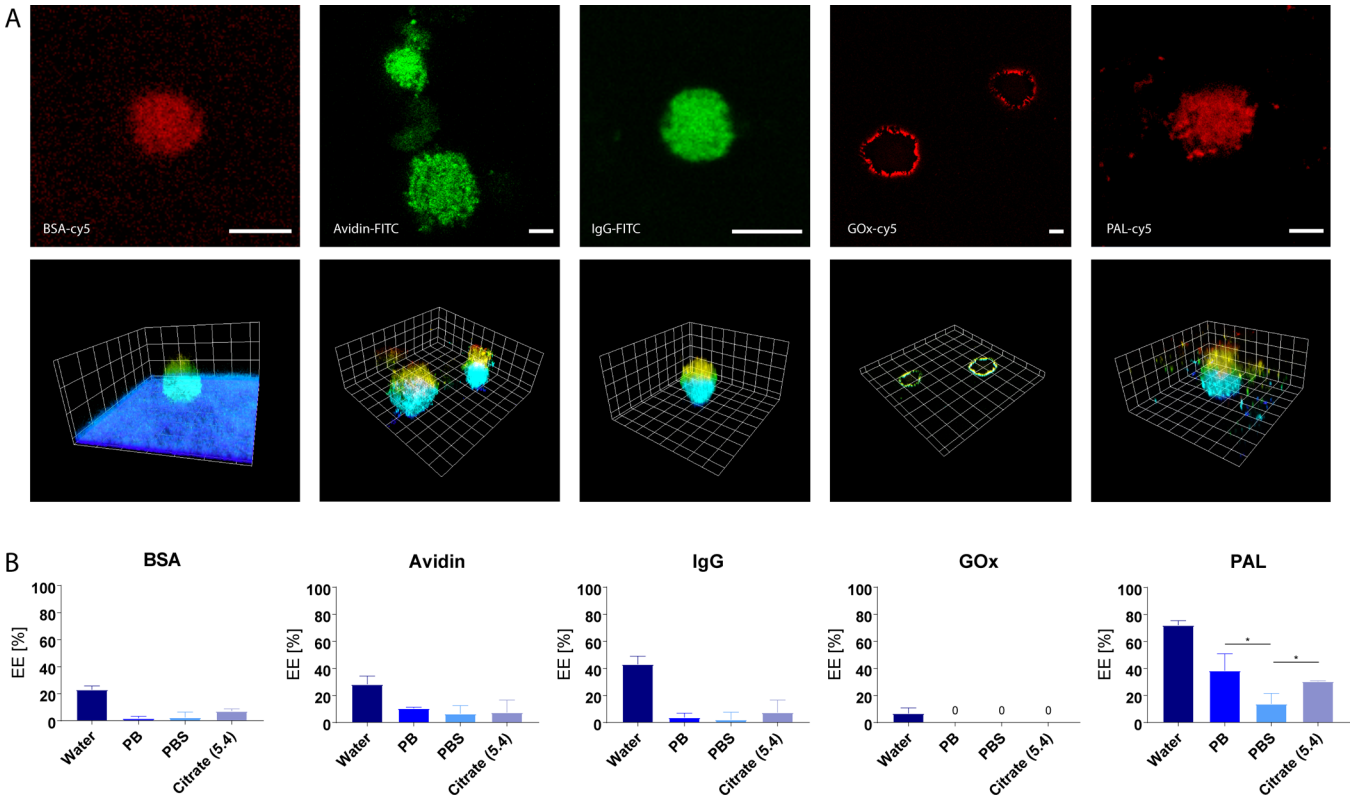

Figure 3. Protein adsorption in porous microparticles. (A) Z-stack confocal microscopy of fluorescent proteins and three-dimensional reconstruction of images. (B) Quantification of protein loading in porous microparticles in water and in three different buffers. Scale bars represent 5 μm. Data presented as mean ± SD ($n \geq 3$).

https://doi.org/10.1021/acsbiomedchemau.3c00001
ACS Bio Med Chem Au 2023, 3, 252−260

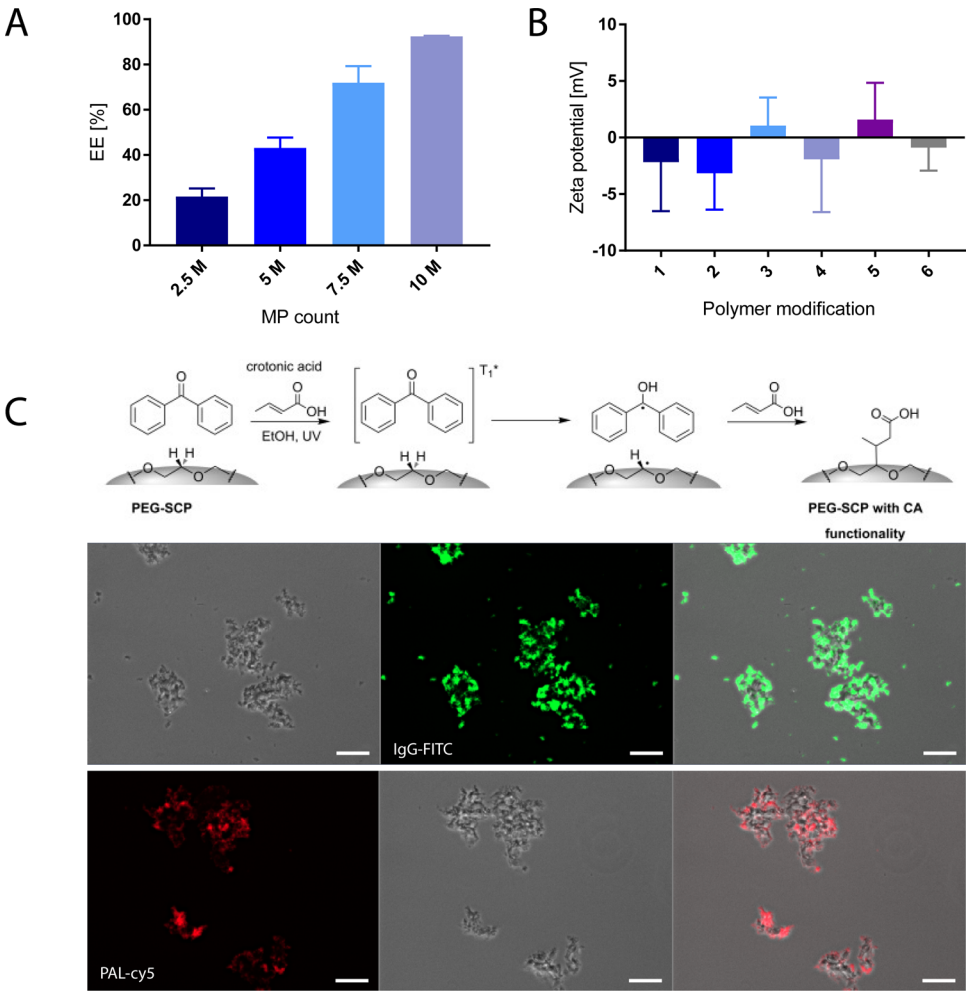

Figure 4. Optimization of protein loading for model protein BSA-FITC. (A) EE of protein with increasing particle/protein ratios. (B) Modification of polymer composition of particles to modulate surface charge and electrostatic interactions. (1. Standard PHMPs; 2. MAETAC 200 mM; 3. MAETAC 300 mM; 4. NH+ 2.5 mol %; 5. NH+ 5 mol %; and 6. DMAEMA (200 mM) + ethyl bromide) (C) Grafting of carboxyl groups on the PEG backbone for EDC/NHS conjugation of proteins (reaction figure from Schmidt et al.,[20] "Probing multivalency in ligand–receptor-mediated adhesion of soft, biomimetic interfaces", *Beilstein J. Org. Chem.* 2015, 10.3762/bjoc.11.82, published by Beilstein-Institut, distributed under the Creative Commons 2.0. attribution license). Scale bars represent 50 μm. Data presented as mean ± SD ($n \geq 3$).

Finally, the correlation between the particle to protein ratio and EE was also evaluated using BSA at 40 μg/mL in water and increasing particle counts (Figure 4A). For the conditions tested, it was revealed that the increase in particle count leads to a direct and proportional increase in EE from 21.5% for 2.5 M particles to 92.5% for 10 M particles. In fact, this trend shows a high degree of linearity with an $R^2 > 0.99$.

Taken together, these results do not reveal a clear pattern of protein adsorption in relation to size or isoelectric point (charge). Proteins interact with hydrogels through a number of nonspecific interactions, which include electrostatic interactions (repulsive or attractive), hydrogen bonding, and van der Waals interactions,[43] which may act synergistically or antagonistically to enhance or decrease protein adsorption. Amino acid composition at the surface of these globular proteins and their potential contribution to interactions with PEG may provide more insight on these differences.

Optimization of Protein Encapsulation

In this study, several strategies to enhance protein encapsulation were investigated. The first approach evaluated was the modulation of the chemical composition of the PHMPs in order to change the particle charge and potentially increase electrostatic interactions with a given protein. One strategy to do this on telechelic PEG hydrogels was reported by Tan et al.,[44] who integrated the positively charged monomer MAETAC into a PEG-diacrylate hydrogel and reported increased adsorption of plasma proteins. The modulation of hydrogel charge to a positive zeta potential could increase protein adsorption at physiological pH for proteins with an isoelectric point below that pH.[43] MAETAC was added at the start of the PHMP synthesis, dissolved with the PEG-dAAm monomer at concentrations of 200 and 300 mM. However, results show no significant change of the zeta potential for both these MPs (Figure 4B), and no difference in EE. As the process for porous hydrogel particles is relatively complex and includes multiple steps which could potentially degrade a product (UV, heat, and low pH), it could be hypothesized that MAETAC is not stable throughout the PHMP fabrication process. Therefore, an alternative, two-step method was investigated. This alternative method uses incorporation of the neutral DMAEMA and subsequent quaternization using ethyl bromide.[45] However, this method did not lead to any significant change in the zeta potential

https://doi.org/10.1021/acsbiomedchemau.3c00001
ACS Bio Med Chem Au 2023, 3, 252–260

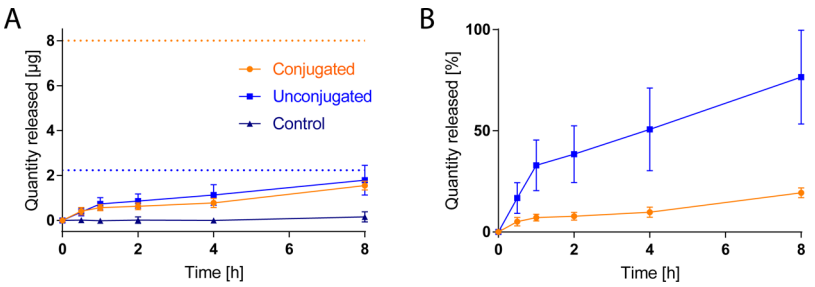

Figure 5. Conjugation of BSA using inclusion of an amine group in PHMP composition. (A) Release of BSA expressed as quantity released [microgram], dotted lines indicate quantity loaded for 10 M particles. (B) Release of BSA expressed as percentage of quantity encapsulated. Data presented as mean ± SD ($n \geq 3$).

(Figure 4B) or protein EE. Finally, a primary amine was included in PHMP composition via a *tert*-butoxycarbonyl (boc)-protected amine attached to a PEG-acrylate moiety (Figure 4B). The boc protecting group is then removed under highly acidic conditions. For all these strategies, results seem to show that while there may be a slight increase in the zeta potential when using modifying polymers at high concentrations (up to 1.6 mV), these changes are not statistically significant and do not increase protein EE.

Alternatively, strategies to conjugate proteins to the PHMPs were also evaluated. The first strategy investigated was previously described by Schmidt et al.,[20,46] who used benzophenone as a photoinitiator for grafting of crotonic acid to the PEG backbone (Figure 4C). While this method was described for PEG-dAAm microparticles, these particles are not identical in structure as they are not porous, are made of higher MW monomers (8 kDA), and do not undergo the same cross-linking mechanism. In fact, results showed that the multiple washing steps, the two solvent exchanges (water to ethanol to water), and EDC/NHC activation led to a loss of a high number of particles. Furthermore, the few particles recovered at the end of this process seemed to have aggregated and lost their spherical morphology (Figure 4C). Although the conjugation seemed successful, as observed by fluorescence microscopy with IgG-FITC and PAL-cy5 (negative controls in Figure S4), the process seemed to be unsuitable for porous PHMPs without some optimization.

Finally, another EDC/NHS conjugation method was investigated, using the carboxyl groups from the protein and incorporating a primary amine in the PHMP structure (as opposed to using a carboxyl on the MP and amine on the protein). To do this, a boc-protected amine attached to a PEG-acrylate moiety was incorporated into PHMP composition at 5 mol %. The amine was then deprotected after PHMP synthesis under acidic conditions. Combining EDC/NHS-activated protein to amine-containing PHMPs led to greater encapsulation compared to a nonconjugated sample in PBS. Indeed, for the 10 M particles used in the experiment, approximately 8 μg of protein was encapsulated, whereas only 2 μg was encapsulated via simple adsorption. Furthermore, the release of encapsulated protein over 8 h showed a maximum release of 19% (1.55 μg) for the conjugated sample versus 77% (1.79 μg) for the nonconjugated sample (Figure 5). As both conjugated and unconjugated formulations display similar release profiles in terms of quantities (microgram) of protein released, it could be hypothesized that the encapsulated protein in the conjugated system can be divided into two subsets: adsorbed protein and conjugated protein. The adsorbed portion of encapsulated proteins would release with similar kinetics to the unconjugated formulation, while the conjugated protein would remain within the PHMPs as it is covalently bound to the hydrogel.

While there are many studies investigating protein-loaded hydrogels, the multitude of factors influencing protein encapsulation, as well as the difference in methodologies make direct comparison difficult. Indeed, the synthesis method, polymer molecular weight and charge, cross-linking process, and mesh size are among the many factors affecting protein loading and release.[47−49] In this study, protein loading in bioconjugated particles equates to approximately 3 μg of protein per mg of polymer, which is considerably lower than what can be achieved through other particle synthesis techniques such as microemulsion or microfluidics,[49−52] which can achieve protein loading quantities upward of 100 μg/mg. However, PHMPs present the advantage of having a postfabrication protein conjugation, making it possible to conjugate many different proteins to their polymeric structure without modifications to the synthesis protocol. Furthermore, we hypothesize that much of the conjugated protein content is located at the surface of the particles, which when combined to the high specific area of the particles granted to them by their porosity could allow for increased protein interactions with therapeutic targets, such as enzymatic substrates or antibody ligands.

Overall, these results show that protein conjugation to PHMPs using incorporation of an amine group in the microgel structure significantly increases protein encapsulation and decreases the percentage of protein released over time. This method could be an interesting tool for increasing protein encapsulation and retention in PHMPs, as our experiments have shown that EE is usually low in buffered media (≤10%). Conjugation of proteins to PHMPs could potentially be applied to delivery of therapeutic enzymes, under the condition that enzymatic activity is preserved after conjugation.

CONCLUSIONS

In this study, we investigated PHMPs as vehicles for the delivery of biologics. These particles are made using hard $CaCO_3$ templates, which required precise optimization to obtain porous microspheres of suitable morphology and size. These templates could then be used to synthesize PHMPs, which were then characterized to evaluate their structure and protein encapsulation potential. Overall, using fluorescent proteins and confocal microscopy, it was established that proteins can be adsorbed throughout the whole particle. Furthermore, encapsulation of proteins in PHMPs revealed that these particles could adsorb a wide variety of proteins with different properties. Indeed, proteins with molecular weights of

https://doi.org/10.1021/acsbiomedchemau.3c00001
ACS Bio Med Chem Au 2023, 3, 252−260

up to 330 kDa and isoelectric points well below and above physiological pH (4.7−10.5) were able to adsorb throughout the particles. However, results show that EE in buffered media is usually low and requires further optimization. To address this, multiple strategies to enhance protein encapsulation and to conjugate protein to PHMPs were investigated. While attempts at modifying PHMP surface charge did not lead to significant changes in particle charge or EE, protein conjugation strategies were more successful. Indeed, using EDC/NHS conjugation, we were able to increase protein encapsulation fourfold and considerably limit protein release over time. The PHMPs evaluated in this study seem to be interesting as a versatile platform for the delivery of proteins such as enzymes or antibodies for diverse biomedical applications.

■ ASSOCIATED CONTENT

Supporting Information

The Supporting Information is available free of charge at https://pubs.acs.org/doi/10.1021/acsbiomedchemau.3c00001.

Additional data, including electron microscopy images of $CaCO_3$ templates and PHMPs, as well as microscopy images of PHMPs of 20 kDa molecular weight (PDF)

■ AUTHOR INFORMATION

Corresponding Author

Davide Brambilla − *Faculté de Pharmacie, Université de Montréal, Montréal, Québec H3T 1J4, Canada;* orcid.org/0000-0002-5749-1125; Email: davide.brambilla@umontreal.ca

Authors

Philippe Delbreil − *Faculté de Pharmacie, Université de Montréal, Montréal, Québec H3T 1J4, Canada;* orcid.org/0000-0001-8550-2066

Xavier Banquy − *Faculté de Pharmacie, Université de Montréal, Montréal, Québec H3T 1J4, Canada;* orcid.org/0000-0002-3342-3179

Complete contact information is available at: https://pubs.acs.org/10.1021/acsbiomedchemau.3c00001

Notes

The authors declare no competing financial interest.

■ REFERENCES

(1) Wichterle, O.; Lím, D. Hydrophilic Gels for Biological Use. *Nature* **1960**, *185*, 117−118.

(2) Peppas, N. A.; Hilt, J. Z.; Khademhosseini, A.; Langer, R. Hydrogels in Biology and Medicine: From Molecular Principles to Bionanotechnology. *Adv. Mater.* **2006**, *18*, 1345−1360.

(3) Lee, K. Y.; Mooney, D. J. Hydrogels for Tissue Engineering. *Chem. Rev.* **2001**, *101*, 1869−1880.

(4) Correa, S.; Grosskopf, A. K.; Lopez Hernandez, H.; Chan, D.; Yu, A. C.; Stapleton, L. M.; Appel, E. A. Translational Applications of Hydrogels. *Chem. Rev.* **2021**, *121*, 11385−11457.

(5) Lewis, K. A.; Eugster, E. A. Experience with the once-yearly histrelin (GnRHa) subcutaneous implant in the treatment of central precocious puberty. *Drug Des., Dev. Ther.* **2009**, *3*, 1−5.

(6) Wang, R.; Guo, K.; Zhang, W.; He, Y.; Yang, K.; Chen, Q.; Yang, L.; Di, Z.; Qiu, J.; Lei, P.; Gu, Y.; Luo, Z.; Xu, X.; Xu, Z.; Feng, X.; Li, S.; Yu, Z.; Xu, H. Poly-γ-Glutamic Acid Microgel-Encapsulated Probiotics with Gastric Acid Resistance and Smart Inflammatory Factor Targeted Delivery Performance to Ameliorate Colitis. *Adv. Funct. Mater.* **2022**, *32*, No. 2113034.

(7) Men, Y.; Peng, S.; Yang, P.; Jiang, Q.; Zhang, Y.; Shen, B.; Dong, P.; Pang, Z.; Yang, W. Biodegradable Zwitterionic Nanogels with Long Circulation for Antitumor Drug Delivery. *ACS Appl. Mater. Interfaces* **2018**, *10*, 23509−23521.

(8) Li, J.; Mooney, D. J. Designing hydrogels for controlled drug delivery. *Nat. Rev. Mater.* **2016**, *1*, 16071.

(9) Peppas, N. A.; Keys, K. B.; Torres-Lugo, M.; Lowman, A. M. Poly(ethylene glycol)-containing hydrogels in drug delivery. *J. Controlled Release* **1999**, *62*, 81−87.

(10) Cao, H.; Duan, L.; Zhang, Y.; Cao, J.; Zhang, K. Current hydrogel advances in physicochemical and biological response-driven biomedical application diversity. *Signal Transduction Targeted Ther.* **2021**, *6*, 426.

(11) Shih, T.-Y.; Blacklow, S. O.; Li, A. W.; Freedman, B. R.; Bencherif, S.; Koshy, S. T.; Darnell, M. C.; Mooney, D. J. Injectable, Tough Alginate Cryogels as Cancer Vaccines. *Adv. Healthcare Mater.* **2018**, *7*, No. 1701469.

(12) Tang, Y.; Lin, S.; Yin, S.; Jiang, F.; Zhou, M.; Yang, G.; Sun, N.; Zhang, W.; Jiang, X. In situ gas foaming based on magnesium particle degradation: A novel approach to fabricate injectable macroporous hydrogels. *Biomaterials* **2020**, *232*, No. 119727.

(13) De France, K. J.; Xu, F.; Hoare, T. Structured Macroporous Hydrogels: Progress, Challenges, and Opportunities. *Adv. Healthcare Mater.* **2018**, *7*, No. 1700927.

(14) Zhou, S.; Bismarck, A.; Steinke, J. H. G. Ion-responsive alginate based macroporous injectable hydrogel scaffolds prepared by emulsion templating. *J. Mater. Chem. B* **2013**, *1*, 4736−4745.

(15) Sackett, S. D.; Tremmel, D. M.; Ma, F.; Feeney, A. K.; Maguire, R. M.; Brown, M. E.; Zhou, Y.; Li, X.; O'Brien, C.; Li, L.; Burlingham, W. J.; Odorico, J. S. Extracellular matrix scaffold and hydrogel derived from decellularized and delipidized human pancreas. *Sci. Rep.* **2018**, *8*, 10452.

(16) Narayanaswamy, R.; Torchilin, V. P. Hydrogels and Their Applications in Targeted Drug Delivery. *Molecules* **2019**, *24*, 603.

(17) Behra, M.; Schmidt, S.; Hartmann, J.; Volodkin, D. V.; Hartmann, L. Synthesis of Porous PEG Microgels Using CaCO3 Microspheres as Hard Templates. *Macromol. Rapid Commun.* **2012**, *33*, 1049−1054.

(18) Babity, S.; Couture, F.; Campos, E. V. R.; Hedtrich, S.; Hagen, R.; Fehr, D.; Bonmarin, M.; Brambilla, D. A Naked Eye-Invisible Ratiometric Fluorescent Microneedle Tattoo for Real-Time Monitoring of Inflammatory Skin Conditions. *Adv. Healthcare Mater.* **2022**, *11*, No. e2102070.

(19) Pussak, D.; Behra, M.; Schmidt, S.; Hartmann, L. Synthesis and functionalization of poly(ethylene glycol) microparticles as soft colloidal probes for adhesion energy measurements. *Soft Matter* **2012**, *8*, 1664−1672.

(20) Schmidt, S.; Wang, H.; Pussak, D.; Mosca, S.; Hartmann, L. Probing multivalency in ligand-receptor-mediated adhesion of soft, biomimetic interfaces. *Beilstein J. Org. Chem.* **2015**, *11*, 720−729.

(21) Trushina, D. B.; Bukreeva, T. V.; Kovalchuk, M. V.; Antipina, M. N. CaCO3 vaterite microparticles for biomedical and personal care applications. *Mater. Sci. Eng., C* **2014**, *45*, 644−658.

(22) Boyjoo, Y.; Pareek, V. K.; Liu, J. Synthesis of micro and nano-sized calcium carbonate particles and their applications. *J. Mater. Chem. A* **2014**, *2*, 14270−14288.

(23) Volodkin, D. V.; Petrov, A. I.; Prevot, M.; Sukhorukov, G. B. Matrix Polyelectrolyte Microcapsules: New System for Macromolecule Encapsulation. *Langmuir* **2004**, *20*, 3398−3406.

(24) Volodkin, D. V.; Schmidt, S.; Fernandes, P.; Larionova, N. I.; Sukhorukov, G. B.; Duschl, C.; Möhwald, H.; von Klitzing, R. One-Step Formulation of Protein Microparticles with Tailored Properties: Hard Templating at Soft Conditions. *Adv. Funct. Mater.* **2012**, *22*, 1914−1922.

(25) Han, Y. S.; Hadiko, G.; Fuji, M.; Takahashi, M. Effect of flow rate and CO_2 content on the phase and morphology of $CaCO_3$ prepared by bubbling method. *J. Cryst. Growth* **2005**, *276*, 541−548.
(26) Donnet, M.; Bowen, P.; Jongen, N.; Lemaître, J.; Hofmann, H. Use of Seeds to Control Precipitation of Calcium Carbonate and Determination of Seed Nature. *Langmuir* **2005**, *21*, 100−108.
(27) Andreassen, J.-P.; Hounslow, M. J. Growth and aggregation of vaterite in seeded-batch experiments. *AIChE J.* **2004**, *50*, 2772−2782.
(28) Parkin, S. J.; Vogel, R.; Persson, M.; Funk, M.; Loke, V. L. Y.; Nieminen, T. A.; Heckenberg, N. R.; Rubinsztein-Dunlop, H. Highly birefringent vaterite microspheres: production, characterization and applications for optical micromanipulation. *Opt. Express* **2009**, *17*, 21944−21955.
(29) Durán, J. D. G.; Ontiveros, A.; Delgado, A. V.; González-Caballero, F.; Chibowski, E. A study on the adhesion of calcium carbonate to glass. Energy balance in the deposition process. *J. Adhes. Sci. Technol.* **1996**, *10*, 847−868.
(30) Frisia, S., Calcium carbonate and the carbonic acid system. In *Geochemistry*; Springer Netherlands: Dordrecht, 1998; pp 51−57.
(31) Temenoff, J. S.; Athanasiou, K. A.; Lebaron, R. G.; Mikos, A. G. Effect of poly(ethylene glycol) molecular weight on tensile and swelling properties of oligo(poly(ethylene glycol) fumarate) hydrogels for cartilage tissue engineering. *J. Biomed. Mater. Res.* **2002**, *59*, 429−437.
(32) Hodge, J. G.; Zamierowski, D. S.; Robinson, J. L.; Mellott, A. J. Evaluating polymeric biomaterials to improve next generation wound dressing design. *Biomater. Res.* **2022**, *26*, 50.
(33) Wang, P.; Fang, J.; Qin, S.; Kang, Y.; Zhu, D.-M. Molecular Weight Dependence of Viscosity and Shear Modulus of Polyethylene Glycol (PEG) Solution Boundary Layers. *J. Phys. Chem. C* **2009**, *113*, 13793−13800.
(34) Peters, T. Serum Albumin. In *The Plasma Proteins*, 2nd ed.), Putnam, F. W., Ed.; Academic Press, 1975; pp 133−181.
(35) Li, R.; Wu, Z.; Wangb, Y.; Ding, L.; Wang, Y. Role of pH-induced structural change in protein aggregation in foam fractionation of bovine serum albumin. *Biotechnol. Rep.* **2016**, *9*, 46−52.
(36) Haugland, R. P.; You, W. W. Coupling of Antibodies With Biotin. In *Avidin-Biotin Interactions: Methods and Applications*, McMahon, R. J., Ed.; Humana Press: Totowa, NJ, 2008; pp 13−23.
(37) Wright, K. Antibodies a laboratory manual: By E Harlow and D Lane. pp 726. Cold Spring Harbor Laboratory. 1988. $50 ISBN 0-87969-314-2. *Biochem. Educ.* **1989**, *17*, 220−220.
(38) Benavidez, T. E.; Torrente, D.; Marucho, M.; Garcia, C. D. Adsorption and catalytic activity of glucose oxidase accumulated on OTCE upon the application of external potential. *J. Colloid Interface Sci.* **2014**, *435*, 164−170.
(39) MacDonald, M. J.; D'Cunha, G. B. A modern view of phenylalanine ammonia lyase. *Biochem. Cell Biol.* **2007**, *85*, 273−282.
(40) Pasche, S.; Vörös, J.; Griesser, H. J.; Spencer, N. D.; Textor, M. Effects of Ionic Strength and Surface Charge on Protein Adsorption at PEGylated Surfaces. *J. Phys. Chem. B* **2005**, *109*, 17545−17552.
(41) Dahal, Y. R.; Olvera de la Cruz, M. Controlling protein adsorption modes electrostatically. *Soft Matter* **2020**, *16*, 5224−5232.
(42) Wang, Y.; He, G.; Li, Z.; Hua, J.; Wu, M.; Gong, J.; Zhang, J.; Ban, L.-T.; Huang, L. Novel Biological Hydrogel: Swelling Behaviors Study in Salt Solutions with Different Ionic Valence Number. *Polymer* **2018**, *10*, 112.
(43) Zustiak, S. P.; Wei, Y.; Leach, J. B. Protein-hydrogel interactions in tissue engineering: mechanisms and applications. *Tissue Eng., Part B* **2013**, *19*, 160−171.
(44) Tan, F.; Xu, X.; Deng, T.; Yin, M.; Zhang, X.; Wang, J. Fabrication of positively charged poly(ethylene glycol)-diacrylate hydrogel as a bone tissue engineering scaffold. *Biomed. Mater.* **2012**, *7*, No. 055009.
(45) Banquy, X.; Burdyńska, J.; Lee, D. W.; Matyjaszewski, K.; Israelachvili, J. Bioinspired Bottle-Brush Polymer Exhibits Low Friction and Amontons-like Behavior. *J. Am. Chem. Soc.* **2014**, *136*, 6199−6202.
(46) Strzelczyk, A. K.; Wang, H.; Lindhorst, A.; Waschke, J.; Pompe, T.; Kropf, C.; Luneau, B.; Schmidt, S. Hydrogel Microparticles as Sensors for Specific Adhesion: Case Studies on Antibody Detection and Soil Release Polymers. *Gels* **2017**, *3*, 31.
(47) Tong, X.; Lee, S.; Bararpour, L.; Yang, F. Long-Term Controlled Protein Release from Poly(Ethylene Glycol) Hydrogels by Modulating Mesh Size and Degradation. *Macromol. Biosci.* **2015**, *15*, 1679−1686.
(48) Vermonden, T.; Censi, R.; Hennink, W. E. Hydrogels for Protein Delivery. *Chem. Rev.* **2012**, *112*, 2853−2888.
(49) Liu, A. L.; García, A. J. Methods for Generating Hydrogel Particles for Protein Delivery. *Ann. Biomed. Eng.* **2016**, *44*, 1946−1958.
(50) Kim, Y.; Sah, H. Protein Loading into Spongelike PLGA Microspheres. *Pharmaceutics* **2021**, *13*, 137.
(51) Yu, L.; Sun, Q.; Hui, Y.; Seth, A.; Petrovsky, N.; Zhao, C.-X. Microfluidic formation of core-shell alginate microparticles for protein encapsulation and controlled release. *J. Colloid Interface Sci.* **2019**, *539*, 497−503.
(52) Rios, J. L.; Lu, G.; Seo, N. E.; Lambert, T.; Putnam, D. Prolonged Release of Bioactive Model Proteins from Anionic Microgels Fabricated with a New Microemulsion Approach. *Pharm. Res.* **2016**, *33*, 879−892.

https://doi.org/10.1021/acsbiomedchemau.3c00001
ACS Bio Med Chem Au 2023, 3, 252−260